

## Resolution in rotation measurements

Stephen M Barnett and Roberta Zambrini

Department of Physics, University of Strathclyde, Glasgow G0 4NG, United Kingdom

(v1.1 14 Feb 2005)

**Abstract.** The limiting resolution in optical interferometry is set by the number of photons used, with the functional dependence determined by the state of light that is prepared. We consider the problem of measuring the rotation of a beam of light about an optical axis and show how the limiting resolution depends on the total number of *quanta of orbital angular momentum* carried by the light beam.

### 1 Introduction

It has long been recognised that the ultimate accuracy of optical measurements is set by the quantum nature of light. Indeed the desire to approach these quantum limits was a strong motivation for the study of nonclassical and particularly squeezed states of light [1]. The use of coherent laser sources typically provides a limiting resolution that is inversely proportional to the square root of the mean number of photons used in the measurement ( $N^{-1/2}$ ). This can be improved upon by the use of squeezed states which enhances the resolution by the square root of the degree of squeezing ( $N^{-1/2}e^{-r}$ ). The full quantum limit is reached by complete control of the photon number and gives a quantum limited resolution that is inversely proportional to the photon number ( $N^{-1}$ ) [2].

One of the earliest proposals for the application of squeezed light was to improve the sensitivity of optical interferometry [3], which was demonstrated very soon after the first successful squeezing experiments [4, 5]. This was followed by a demonstration of enhanced sensitivity in a spectroscopic measurement [6]. More recently, it has been suggested that squeezed light can be used to enhance the resolution of measurements of small displacements in optical images, or beam displacements [7]. An experimental demonstration, based on squeezed light prepared in a novel ‘flipped’ mode, followed soon afterwards [8].

The quantum limit for detection of phase shifts can be approached using a balanced interferometer with equal intensity inputs [9]. It has also been

arXiv:quant-ph/0503224v1 30 Mar 2005

suggested that the same degree of resolution could be achieved by means of special beam-splitters that send all of the light through one arm of the interferometer so that a two-mode ‘Schrödinger-cat’ state is prepared [10,11]. The same  $N^{-1}$ -limited resolution can be obtained for beam displacements by use of a pair of specially shaped modes, each having precisely the same number of photons [12].

In this paper we examine the factors limiting our ability to measure the rotation of a beam about the optical axis. We will find that, as with interferometric and beam-displacement measurements, the resolution depends on the number of photons used and can be improved by the use of suitable nonclassical states of light. The resolution also depends, however, on the orbital angular momentum of the light used to make the observation [13,14]. We will find that it is the product of the orbital angular momentum per photon,  $\hbar\ell$ , and the total photon number,  $N$ , that determines the limiting resolution. Hence it is the total number of quanta of orbital angular momentum,  $N\ell$ , that sets the minimum detectable rotation.

After some general considerations, Sect. 2, we present two different schemes to measure small rotations, Sect. 3 and Sect. 4. A comparison of the resolution achievable by different measurements concludes the paper, Sect. 5.

## 2 General considerations

Let us consider a light beam propagating through an *image rotator*, that is a device that rotates an input image about the optical axis. It is not necessary to specify the form of the rotator, but elementary examples include a rotating Dove prism [15], or a pair of stationary Dove prisms with a fixed relative orientation. The latter arrangement has recently been used to detect optical angular momentum at the single-photon level [16]. A further example of a beam rotator is a light beam passing *off-axis* through a rotating glass disc, which induces a tangential displacement, or rotation, of the beam [17]<sup>1</sup>.

In this work we consider a beam with an image, or transverse spatial profile,  $u_I(x, y)$  propagating in the  $z$  direction through an image rotator. The beam after passing through the rotator has a transverse profile

$$u_O(x, y) = u_I(x \cos \delta\phi + y \sin \delta\phi, y \cos \delta\phi - x \sin \delta\phi), \quad (1)$$

where  $\delta\phi$  is the azimuthal rotation angle and we fix the  $z$  axis as the rotation axis. In Sect. 3 and 4 we will consider two different beams  $u_I$ .

---

<sup>1</sup>It has recently been suggested that the dual phenomenon, i.e. light carrying orbital angular momentum exerting a torque on a transparent medium, should also exist [18].

It is natural to describe the beam  $u_I$  as superposition of Laguerre-Gaussian modes as these are eigenmodes of the  $z$ -component of angular momentum, which is the generator of the rotation. This means that the only effect of a rotator on these modes is to add a constant phase shift. Laguerre-Gaussian modes, which at the beam waist have the form [19]:

$$u_{p\ell}(r, \phi) = \frac{1}{w_0} \sqrt{\frac{p!}{\pi(|\ell| + p)!}} \exp\left[-\frac{r^2}{2w_0^2}\right] \left(\frac{r}{w_0}\right)^{|\ell|} L_p^{|\ell|}\left(\frac{r^2}{w_0^2}\right) e^{i\ell\phi}, \quad (2)$$

are labelled by an angular index,  $\ell$ , associated with the angular momentum carried by the beam [13], and by a radial index,  $p$ , giving  $p + 1$  bright rings in the intensity profile (Fig. 1). Modes with  $p = 0$  have a single intense ring with radius [20]

$$\bar{r} = w_0 \sqrt{|\ell|}. \quad (3)$$

Modes with non-vanishing  $p$  have a less compact spatial distribution in the transverse plane (see Fig. 1c-d).

Our study of rotation measurements starts with the realization that the optics used will, inevitably, have a maximum distance from the optical axis beyond which light will be lost by the experiment. For simplicity, we suppose that this limit is set by the radius  $R$  of the rotator. This, in turn, sets a maximum value for the angular momentum that can be carried by a mode propagating through it [21]. The Laguerre-Gaussian modes with non-zero  $p$  extend to a larger radius than those with the same value of  $\ell$  but  $p = 0$  (see Fig. 1). This means that the largest allowed angular momentum will occur for a  $p = 0$  mode. For a mode with a bright ring of radius (3) at the edges of the device ( $\bar{r} = R$ ), the beam would be strongly diffracted. The radial intensity distribution of the Laguerre-Gaussian modes, for large values of  $|\ell|$ , has the form

$$|u_{0\ell}(\bar{r} + d)|^2 \simeq |u_{0\ell}(\bar{r})|^2 e^{-d^2/w_0^2}, \quad (4)$$

so that the intensity tends to be radially distributed like a Gaussian centred in  $\bar{r}$  and with a waist  $w_0$ . Hence we can set the limit for a transmitted Laguerre-Gaussian mode for

$$\bar{r} + w_0 = R. \quad (5)$$

From Eq. (3) we obtain the maximum angular momentum index transmitted

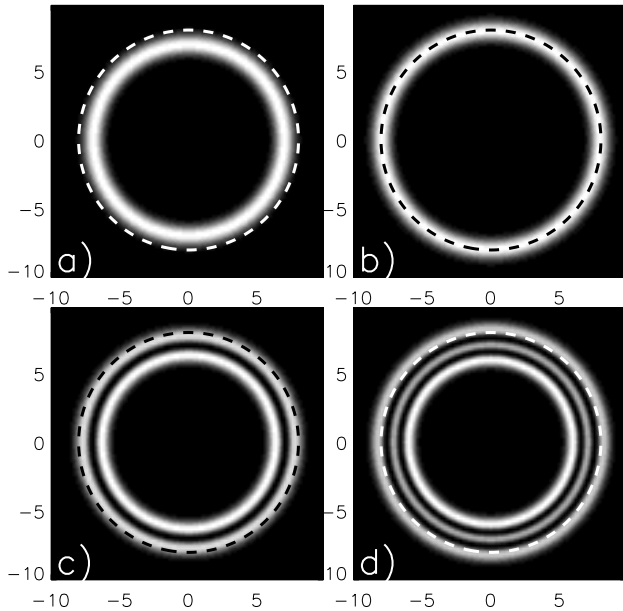


Figure 1. Intensity  $\left(\rho^{|\ell|} e^{-\frac{\rho^2}{2}} L_p^{|\ell|}(\rho^2)\right)^2$ , with radial coordinate normalized with the beam waist  $\rho = r/w_0$ . The dashed circle, with radius 8 represents the transverse extension of a rotator. Beams with  $p = 0$  have the maximum intensity at  $\rho = \sqrt{|\ell|}$ . a) Intensity for  $\ell = 49$ ,  $p = 0$ , showing a bright circle with radius 7. b) For the mode  $\ell = 64$ ,  $p = 0$  the maximum intensity is at the boundary of the device. For increasing value of  $p$  we observe a spreading in the intensity, as shown in c)  $\ell = 49$ ,  $p = 1$  and d)  $\ell = 49$ ,  $p = 2$ .

by a device with maximum effective radius  $R$  as:

$$\ell_M = \left(\frac{R}{w_0} - 1\right)^2. \quad (6)$$

We can use this result to suggest a probable limit for the smallest detectable rotation  $\delta\phi$ . Consider the uncertainty relation for rotation angle and angular momentum [22]

$$\Delta\phi\Delta L \geq \frac{\hbar}{2}|1 - 2\pi P(\pi)|, \quad (7)$$

where the values of  $\phi$  are in the range  $[-\pi, \pi]$ . The form of this uncertainty relation has recently been confirmed experimentally [23], and states minimizing the uncertainty product (7) have been derived [24]. For small angular

uncertainties we have

$$\Delta\phi \geq \frac{\hbar}{2\Delta L}, \quad (8)$$

which gives a bound on the minimum possible  $\Delta\phi$ :

$$\Delta\phi \geq \frac{1}{2\ell_M}. \quad (9)$$

For the analogous problem of the optical phase [25] the minimum achievable uncertainty is inversely proportional to the mean (or maximum) photon number ( $N$ ) [26]. The minimum resolvable phase shift also seems to be inversely proportional to  $N$  [9, 12]. This suggests that the minimum resolvable rotation given a single photon will be

$$\delta\phi \propto \ell_M^{-1}. \quad (10)$$

We expect that the optimal use of  $N$  photons will give a limit

$$\delta\phi \propto (N\ell_M)^{-1}. \quad (11)$$

The analogy between the uncertainty,  $\Delta\phi$ , and the resolution,  $\delta\phi$ , leads us to refer to (11) as the ‘Heisenberg’ limit.

### 3 Displacement scheme

A natural way to measure small angles imparted by an image rotator is through the displacement of a beam shining the rotator far from the axis, as in Jones experiment [17]. In this scheme the azimuthal displacement gives the measure of the rotation angle, as shown in Fig. 2. Clearly the resolution is increased by working at the edges of the device, that is at the maximum distance from the device axis, and with a small size of the light spot. In the following we consider a beam with a Gaussian transverse profile, centred in  $x = r_0, y = 0$

$$u_I(x, y) = \frac{1}{\pi^{1/2}w_0} \exp \left[ -\frac{(x - r_0)^2 + y^2}{2w_0^2} \right], \quad (12)$$

with a small beam waist  $w_0$  and large  $r_0$ , ‘near’ to the edge of the device. Clearly there are limits for the achievable experimental precision due simply to the finite size of the optical elements used. Given a device with a radial size  $R$ , then the off-axis Gaussian (12) will be transmitted if  $r_0 + w_0 \sim R$ .

Figure 2. Scheme based on displacement measurement (picture NA).

The rotated output beam obtained by Eqs. (1) and (12) is

$$u_O(x, y) = \frac{1}{\pi^{1/2}w_0} \exp \left[ -\frac{(x - r_0 \cos \delta\phi)^2 + (y - r_0 \sin \delta\phi)^2}{2w_0^2} \right]. \quad (13)$$

The effect of the rotation is to displace the output beam by  $\Delta x = [r_0^2(\cos \delta\phi - 1)^2 + r_0^2 \sin^2 \delta\phi]^{1/2}$ . For small  $\delta\phi$  we find

$$\delta\phi = \frac{\Delta x}{r_0}, \quad (14)$$

so that the resolution achieved measuring small angles in this scheme depends on the lateral beam position  $r_0$  and on the precise measurement of the displacement  $\Delta x$  between the input and the rotated light spots.

Small displacements  $\Delta x$  are measured with high resolution by shining a split detector and taking the difference of the light intensities on the two halves [7]. For a perfectly aligned beam the signal detected is zero, while any small misalignment gives an imbalance in the intensities. Given a Gaussian mode in a coherent state with mean photon number equal to  $N$ , the minimum displacement measurable is

$$\Delta x = \frac{\sqrt{\pi}w_0}{2} \frac{1}{\sqrt{N}}. \quad (15)$$

The standard quantum limit (15) can be beaten by engineering the spatial mode impinging on the detector and its statistics. In particular the input beam is prepared by superposing an even Gaussian mode (12) with an odd *flipped* mode  $u_I^{odd}(x, y) = u_I(x, y)\text{sign}(y)$ . We note that a flipped mode is not stable under propagation as it has a discontinuity in  $y = 0$  that would be smoothed by diffraction. Nevertheless, it was experimentally possible to beat the shot noise limit in displacement measurements by shaping this kind of beam [8].

In general we have [12]

$$\Delta x = \frac{\sqrt{\pi}w_0}{2} f(N) \quad (16)$$

with  $f(N)$  depending on the state in which the modes  $u_I^{odd}$  and  $u_I$  are prepared. If the Gaussian mode is in a coherent state with average intensity  $N$  and the

flipped mode is in vacuum then  $f(N) = N^{-1/2}$ , as in Eq. (15). This is the limit resolution obtained with classical states, i.e. the standard quantum limit. Better resolution can be achieved if the flipped mode is prepared in a strongly squeezed state, leading to  $f(N) = N^{-3/4}$ . The best resolution is obtained with highly non-classical states, for instance by preparing the two modes in number states  $|N/2\rangle$ . In this case  $f \sim N^{-1}$  and the displacement  $\Delta x \sim N^{-1}$  is the ‘Heisenberg limit’ mentioned in the previous Section.

From these results for displacement measurements we obtain the maximum angle resolution of the scheme in Fig. 2:

$$\delta\phi = \frac{\sqrt{\pi}w_0}{2r_0}f(N). \quad (17)$$

Clearly,  $\delta\phi$  depends both on the spatial characteristics of the mode ( $w_0$  and lateral displacement  $r_0$ ) and also on the state of light (through  $f(N)$ ). A decomposition of (12) in angular momentum eigenmodes allows us to write  $\delta\phi$  in terms of the angular momentum index  $\ell$ . In particular for a Gaussian spot centred far from the axis  $z$  ( $r_0 \gg w_0$ ) there is a large dispersion in the angular momentum spectrum. We can see this either by writing  $u_I(x, y)$  in terms of its angular Fourier components [27]

$$u_I(x, y) = \frac{1}{\pi^{1/2}w_0} \exp\left(-\frac{x^2 + y^2 + r_0^2}{2w_0^2}\right) \sum_{\ell=-\infty}^{\ell=+\infty} I_{|\ell|} \left(\frac{r_0\sqrt{x^2 + y^2}}{w_0^2}\right) e^{i\ell\phi} \quad (18)$$

or by explicitly constructing its decomposition in terms of the Laguerre-Gaussian modes (see Fig. 3b). The latter procedure is carried out in the Appendix. Due to the dispersion in the angular momentum spectrum, it is important to consider the constraint, imposed by the extension  $R$  of the rotator, found in Sect. 2. From Eq. (6) and setting  $r_0 + w_0 = R$  we find the maximum resolution in the displacement scheme

$$\delta\phi = \frac{\sqrt{\pi}}{2} \frac{1}{\sqrt{\ell_M}} f(N). \quad (19)$$

In Eq. (19) we immediately identify a ‘geometrical’ factor depending on the angular momentum index and the statistical factor  $f$ . In analogy with the standard quantum limit, obtained by using Gaussian coherent states in interferometry, we consider the dependence  $\sim 1/\sqrt{\ell}$  in Eq. (19) as the standard *optical* limit for rotation measurements, as it is obtained with Gaussian spatial distributions. A spatial Gaussian mode prepared in a Gaussian coherent state then gives a combined ‘standard quantum limit’ in which the minimum

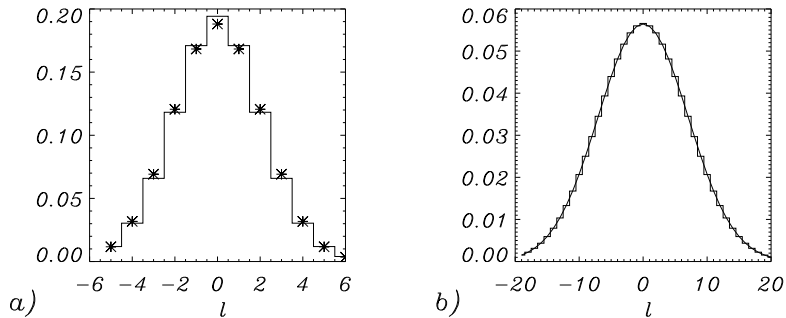


Figure 3. The histograms show the probabilities  $P(\ell)$  given in Eq. (A6). The symbols (a) and smooth line (b) are Gaussians with width given by the variance  $\Delta\ell = r_0/\sqrt{2}w_0$ . a)  $r_0 = 3w_0$ . b)  $r_0 = 10w_0$ .

Figure 4. Interferometric phase measurement using angular momentum eigenstates. The single mode annihilation operators are  $\hat{a} = \int d\vec{x} v_I(\vec{x}) \hat{a}(\vec{x})$ ,  $\hat{b} = \int d\vec{x} v_I(\vec{x}) \hat{b}(\vec{x})$ , where  $\hat{a}(\vec{x})$  and  $\hat{b}(\vec{x})$  are continuum annihilation operators [30]. (picture NA)

resolvable rotation,  $\propto (N\ell_M)^{-1/2}$ , is the inverse of the root square of the number of quanta of angular momentum. For  $r_0 \gg w_0$ , the Gaussian mode becomes a good approximation to an angle-angular momentum minimum uncertainty product state [24] with  $\langle \ell \rangle = 0$ ,  $\Delta\ell = r_0/\sqrt{2}w_0 = \sqrt{\ell_M/2}$  and  $\Delta\phi = 1/\sqrt{2\ell_M}$ . In Fig. 3 the  $P(\ell)$  are plotted for  $r_0 = 3w_0$  and  $r_0 = 10w_0$  and are compared with Gaussians having the same variance. The approach to a Gaussian form is an indication of reaching the minimum uncertainty product limit [24].

#### 4 Interferometric scheme

If the incoming beam is an angular momentum eigenstate then the only effect of the rotator is to add a constant phase shift. Interferometers form the basis of phase shift measurements [28] and so it is natural to consider the interferometer shown in Fig. 4 to measure rotations. The rotator is placed along one of the paths inside the interferometer. Here the shift is in the azimuthal spatial profile of the field and this contrasts with well-known interferometers [29] designed to measure shift in the longitudinal phase of the light beam.

Given any mode of the form

$$v_I(x, y) = v(r) \exp(i\ell\phi) \quad (20)$$



entering in the rotator, the beam at the output will be

$$v_O(x, y) = v_I(x, y) \exp(i\ell\delta\phi). \quad (21)$$

We note that the interferometer considered here has recently been used to detect the angular momentum of single photons [16]. In the context of rotation resolution, we are interested in the smallest angles  $\delta\phi$  that can be measured with this device.

The rotation through an angle  $\delta\phi$  on the beam (20) introduces only a homogeneous phase shift  $\ell\delta\phi$  on the whole beam, and so it follows that the description of the interferometer in Fig. 4 – illuminated by angular momentum eigenmodes – is completely equivalent to standard interferometers [29] measuring longitudinal phase shifts. We note that to have interference the input modes  $a$  and  $b$  need to have the same angular momentum index ( $\ell$ ).

The difference in the intensities of the two beams emerging from the interferometer depends both on the phase shift, here  $\ell\delta\phi$ , and on the quantum state of the incoming beams. In particular, when the noise level has the size of the signal we are at the limit of the smallest detectable phase shift

$$\delta\phi = \frac{1}{\ell} f(N), \quad (22)$$

with  $f(N) = N^{-1/2}, N^{-3/4}, N^{-1}$  depending on the input states of the modes  $a$  and  $b$ . We have seen in Sect. 2 how the transverse size of the device sets the limit of the maximum value of  $\ell$  of the beam that can be transmitted. By using the maximum allowed angular momentum we reach the limiting angle resolution  $\propto 1/\ell_M$ .

It is particularly interesting to consider the case in which the beams entering in the interferometer are prepared in the states  $|N/2\rangle|N/2\rangle$  [9, 12]. The angle resolution is then

$$\delta\phi = 2.24 \frac{1}{\ell_M N}, \quad (23)$$

which is the ‘Heisenberg limit’ anticipated in Section 2.

## 5 Conclusions

The resolution attainable in an optical measurement of rotations,  $\delta\phi$ , depends on two factors, the number of photons and the orbital angular momentum content of the beam. For a displaced Gaussian spot we find, for a single photon, that  $\delta\phi \propto \ell_M^{-1/2}$  where  $\ell_M$  is the largest angular momentum index supportable

by the image rotator. If the measurement is performed by using a coherent state with mean photon number  $N$  than we find that  $\delta\phi \propto (N\ell_M)^{-1/2}$ , i.e., that it is inversely proportional to the square root of the number of quanta of angular momentum. Use of nonclassical states of light can enhance the sensitivity by changing the functional dependence on  $N$ . In particular, use of correlated number states can produce a resolution that is proportional to  $N^{-1}$ . We can also increase the sensitivity by changing the functional dependence on  $\ell_M$ . Using eigenmodes of orbital angular momentum leads to a resolution proportional to  $\ell_M^{-1}$ , with the ultimate ‘Heisenberg’ limit being  $\propto (N\ell_M)^{-1}$ .

We have demonstrated a clear analogy between orbital angular momentum in rotation measurements and photon number in interferometry. There are, however, very important practical differences. Creating states of well defined orbital angular momentum is relatively straightforward, while making photon number states is very difficult. Secondly, enhancement of resolution based on controlling the photon number requires extremely high efficiencies of photon detection as any losses rapidly degrade the signal by changing the expected photon number. Using eigenmodes of orbital angular momentum, however, is relatively robust as no matter how many photon are lost, each of the remaining photons still carries  $\ell\hbar$  units of angular momentum.

## 6 Acknowledgements

This work was supported by the Engineering and Physical Sciences Research Council (GR/S03898/01).

## References

- [1] LOUDON, R., and KNIGHT, P. L., 1987, *J. mod. Opt.*, **34**, 709 and references therein.
- [2] GIOVANNETTI, V., LLOYD, S., MACCONE, L., 2004, *Science*, **306**, 1330.
- [3] CAVES, C. M., 1981, *Phys. Rev. D*, **23**, 1693.
- [4] XIAO, M., WU, L.-A., and KIMBLE, H. J., 1987, *Phys. Rev. Lett.*, **59**, 278.
- [5] GRANGIER, P., SLUSHER, R. E., YURKE, B., and LAPORTA, A., 1987, *Phys. Rev. Lett.*, **59**, 2153.
- [6] POLZIK, E. S., CARRI, J., and KIMBLE, H. J., 1992, *Phys. Rev. Lett.*, **68**, 3020.
- [7] FABRE, C., FOUET, J. B., and MAÎTRE, A., 2000, *Opt. Lett.*, **25**, 76.
- [8] TREPS, N., ANDERSEN, U., BUCHLER, B., LAM, P.K., MAÎTRE, A., BACHOR, H.-A., FABRE, C., 2002, *Phys. Rev. Lett.*, **88**, 203601
- [9] HOLLAND, M. J., and BURNETT, K., 1993, *Phys. Rev. Lett.*, **71**, 1355.
- [10] JACOBSON, J., BJÖRK, G., CHUANG, I., and YAMAMOTO, Y., 1995, *Phys. Rev. Lett.*, **74**, 4835.
- [11] BARNETT, S. M., IMOTO, N., and HUTTNER, B., 1998, *J. mod. Opt.*, **45**, 2217.
- [12] BARNETT, S.M., FABRE, C., MAÎTRE, A., 2003, *European Phys. J. D*, **22**, 513
- [13] ALLEN, L., BEIJERSBERGEN, M. W., SPREEUW, R. J. C., and WOERDMAN, J. P., 1992, *Phys. Rev. A*, **40**, 8185.
- [14] ALLEN, L., BARNETT, S. M., and PADGETT, M. J., 2003, *Optical Angular Momentum* (Bristol: Institute of Physics).
- [15] E.HECHT, 2002, *Optics*, 4<sup>th</sup> ed. (San Francisco: Addison Wesley); Sect. 5.5.2.

- [16] LEACH, J., PADGETT, M. J., BARNETT, S. M., FRANKE-ARNOLD, S. and COURTIAL, J., 2002 *Phys. Rev. Lett.*, **88**, 257901.
- [17] JONES, R. V., 1972, *Proc. R. Soc. Lon. A*, **328**, 337.
- [18] PADGETT, M., BARNETT, S. M. and LOUDON, R. , 2003, *J. mod. Opt.*, **50**, 1555.
- [19] SIEGMAN, A. E., 1986, *Lasers* (Mill Valley: University Science Books).
- [20] ALLEN, L., PADGETT, M., 2000 *J. Opt. Commun.* **184**, 67.
- [21] ZAMBRINI, R., THOMSON, L. C., BARNETT, S. M., PADGETT, M., *J. mod. Opt.*, in press.
- [22] BARNETT, S. M. and PEGG, D. T., 1990, *Phys. Rev. A*, **41** 3427.
- [23] FRANKE-ARNOLD, S., BARNETT, S. M., YAO, E., LEACH, J., COURTIAL, J., PADGETT, M. J., 2004, *New J. Phys.* , **6**, 103.
- [24] PEGG, D. T., BARNETT, S. M., ZAMBRINI, R., FRANKE-ARNOLD, S. , PADGETT, M., *New J. Phys.* in press.
- [25] PEGG, D. T. and BARNETT, S. M., 1989 *Phys. Rev. A*, **39** 1665; PEGG, D. T. and BARNETT, S. M., 1989, *J. mod. Optics*, **36**, 7.
- [26] SUMMY, G.S. AND PEGG, D.T. 1990, *Opt. Commun.*, **77**, 75.
- [27] VASNETSOV, M. V., PAS'KO, V. A., and SOSKIN, M. S., 2004 *New J. Phys*, **7**, 46.
- [28] LOUDON, R., 2000, *The Quantum Theory of Light, 3rd edn.* (Oxford University Press, Oxford).
- [29] YURKE, B., L. MCCALL, S. AND KLAUDER J. R., 1986, *Phys. Rev. A*, **33**, 4033
- [30] GATTI, A., WIEDEMANN, H., LUGIATO, L. A., MARZOLI, I., OPPO, G.-L. and BARNETT, S. M., 1997, *Phys. Rev. A*, **56**, 877.
- [31] ABRAMOWITZ, M., and STEGUN, I. A. (eds.), 1970, *Handbook of Mathematical Functions* (New York: Dover).
- [32] ABRAMOCHKIN, E., and VOLOSTNIKOV, V., 1991, *Opt. Commun.*, **83**, 123.

## Appendix A: Laguerre-Gaussian expansion of a displaced Gaussian beam

We require the expansion of our displaced Gaussian mode (12) in terms of the complete set of Laguerre-Gaussian modes: that is we wish to write (at the beam waist)

$$u_I(x, y) = \sum_{\ell=0}^{\infty} \sum_{p=0}^{\infty} c_{p\ell} u_{p\ell}(r, \phi), \quad (\text{A1})$$

where  $x = r \cos \phi$ ,  $y = r \sin \phi$  and  $u_{p\ell}(r, \phi)$  are the normalised Laguerre-Gaussian modes (2). We find the amplitudes  $c_{p\ell}$  by writing both the displaced Gaussian and the Laguerre-Gaussians as sums of Hermite-Gaussians and then evaluate their overlap using the properties of Hermite polynomials. The displaced Gaussian can be written in the form

$$\begin{aligned} u_I(x, y) &= \frac{1}{\pi^{1/2} w_0} \exp \left[ -\frac{(x^2 + y^2)}{2w_0^2} \right] \exp \left[ \frac{r_0 x}{w_0^2} - \frac{r_0^2}{2w_0^2} \right] \\ &= \frac{1}{\pi^{1/2} w_0} \exp \left[ -\frac{r^2}{2w_0^2} \right] \exp \left[ -\frac{r_0^2}{4w_0^2} \right] \sum_{n=0}^{\infty} \frac{1}{n!} \left( \frac{r_0}{2w_0} \right)^n H_n \left( \frac{x}{w_0} \right) \end{aligned} \quad (\text{A2})$$

where we have used the generating function for Hermite polynomials [31]. The Laguerre-Gaussian modes, with  $\ell \geq 0$ , can be written in the form [32]

$$u_{p\ell}(r, \phi) = \frac{(-1)^p}{2^{2p+\ell} w_0} \sqrt{\frac{1}{\pi(|\ell| + p)! p!}} \exp\left[-\frac{r^2}{2w_0^2}\right] \\ \times \sum_{k=0}^{\ell+2p} (2i)^k P_k^{(\ell+p-k, p-k)}(0) H_{\ell+2p-k}\left(\frac{x}{w_0}\right) H_k\left(\frac{y}{w_0}\right), \quad (\text{A3})$$

where

$$P_k^{(n-k, m-k)}(0) = \frac{(-1)^k}{2^k k!} \left. \frac{d^k}{dt^k} [(1-t)^n (1+t)^m] \right|_{t=0}. \quad (\text{A4})$$

The expansion for negative values of  $\ell$  can be obtained by complex conjugation. We can calculate the coefficients  $c_{p\ell}$  using equations (A2) and (A3) together with the orthogonality properties of the Hermite polynomials:

$$c_{p\ell} = \int_{-\infty}^{\infty} \int_{-\infty}^{\infty} u_{p\ell}^* u_I dx dy \\ = (-1)^p \sqrt{\frac{1}{(|\ell| + p)! p!}} \left(\frac{r_0}{2w_0}\right)^{2p+|\ell|} \exp\left(-\frac{r^2}{4w_0^2}\right). \quad (\text{A5})$$

The modulus squared of these amplitudes are plotted in Fig. A1, for  $r_0/w_0 = 3$  and 10.

It is straightforward to find the fractional power in a displaced Gaussian beam associated with each value  $\ell$ , or equivalently the probability,  $P(\ell)$ , that a single photon will be found to have angular momentum  $\hbar\ell$ :

$$P(\ell) = \sum_{p=0}^{\infty} |c_{p\ell}|^2 = \exp\left(-\frac{r^2}{2w_0^2}\right) I_{|\ell|}\left(\frac{r^2}{2w_0^2}\right), \quad (\text{A6})$$

where  $I_n$  is the modified Bessel function of order  $n$  [31]. That this probability distribution is normalised follows from the property:

$$e^z = I_0(z) + \sum_{n=0}^{\infty} I_n(z). \quad (\text{A7})$$

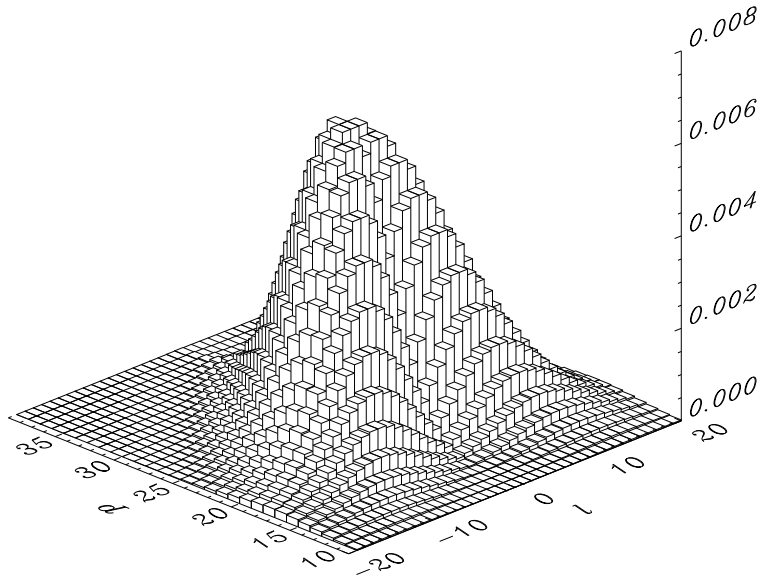
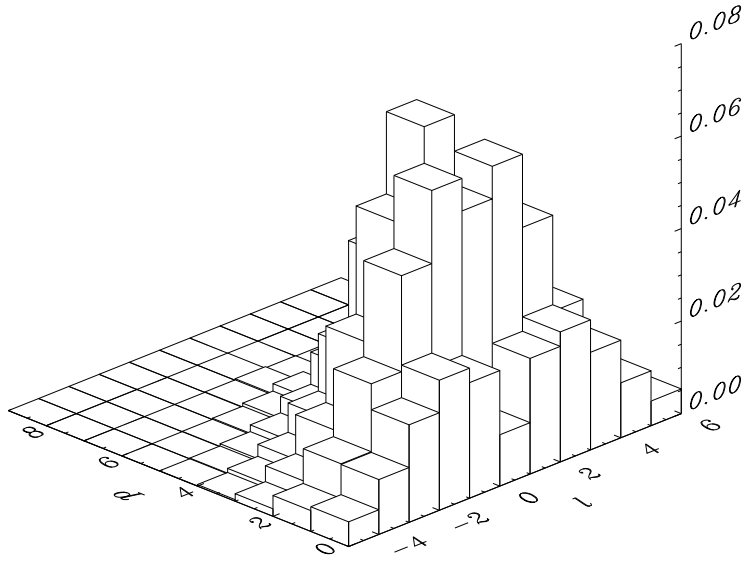


Figure A1. Probabilities  $|c_{p\ell}|^2 = \frac{\exp(r_0^2/2w_0^2)}{(|\ell|+p)!p!} \left(\frac{r_0}{2w_0}\right)^{4p+2|\ell|}$ . Parameter  $r_0/w_0 = 3$  and 10.